Acceleration of Antarctic Circumpolar Current at the Drake Passage during the GRACE era

Chengcheng Yang[1], Xuhua Cheng[1, 2]*, Duotian Huang[1], Jianhuang Qin[1, 2], Guidi Zhou[1], Jiajia Chen[1]

[1]Key Laboratory of Marine Hazards Forecasting, Ministry of Natural Resources, Hohai University, Nanjing, China,

[2]Southern Marine Science and Engineering Guangdong Laboratory(Zhuhai), Zhuhai, China.

*Corresponding author: Xuhua Cheng (xuhuacheng@hhu.edu.cn)

Address: No.1 Xikang Road, Hohai University, Nanjing, China 210098

Key Points:

- The GRACE CSR mascon product can well represent ACC transport at the Drake Passage
- The ACC transport at the Drake Passage has been accelerating during the GRACE era.
- The ACC acceleration can be explained by intensified westerly winds and loss of land ice.

Abstract

Previous studies have identified intense climatic change in the Southern Ocean. However, the response of ACC transport to climate change is not fully understood. In this study, by using in-situ ocean bottom pressure (OBP) records and five GRACE products, long-term variations of ACC transport are studied. Our results confirm the reliability of GRACE CSR mascon product in ACC transport estimation at the Drake Passage. Superimposed on interannual variability, ACC transport exhibits an obvious increasing trend (1.32 ± 0.07Sv year^{-1}) during the GRACE era. Based on results of a mass-conservation ocean model simulation, we suggest that the acceleration of ACC is associated with intensified westerly winds and loss of land ice in Antarctica.

Plain Language Summary

The Southern Ocean is one of the regions most affected by global climatic change. As the dominant circulation in the Southern Ocean, the Antarctic Circumpolar Current (ACC) connects ocean basins, regulating the global climate system and the biogeochemical cycles. However, few studies have explored the response of ACC transport to climate change. In this study, by using OBP data from GRACE satellites, we found that the ACC is accelerating at the Drake passage, due to a combination of intensified westerly winds and loss of land ice in Antarctica.

1. Introduction

The Antarctic Circumpolar Current (ACC), composed of a series of oceanic fronts and a strong eddy field (Figure 1), plays a vital role in regulating the climate system and the carbon cycle (*Meredith et al.*, 2011; *Rintoul*, 2018). Recent studies have identified severe climatic change in the Southern Ocean, manifested in, e.g., subsurface warming (*Roemmich et al.*, 2015), surface freshening (*Haumann et al.*, 2016), and intensified westerly winds (*Thompson et al.*,

2011). Thus, it is valuable to explore the response of ACC transport to climatic change in the Southern Ocean.

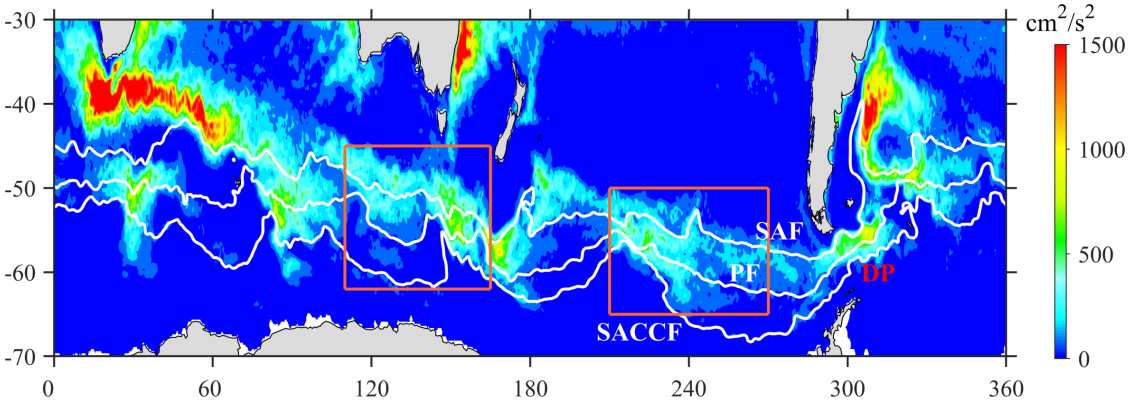

Figure 1. Eddy kinetic energy (EKE) calculated using sea surface height anomalies from AVISO data. White contours denote the Subantractic Front (SAF), Polar Front (PF) and Southern ACC Front (SACCF), respectively. Orange boxes define the areas studied later: 110°-170°E, 45°-62°S in the Indian Ocean and 150°-90°W, 50°-65°S in the Pacific. DP denotes the location of the Drake Passage.

Based on geostrophic balance, previous studies have investigated the variations of ACC transport by using in-situ ocean bottom pressure (OBP) records since 1980s (*Wearn and Baker*, 1980; *Whitworth et al.*, 1982). The Drake Passage, the narrowest constriction of the ACC, has relatively rich bottom pressure recorders. Based on these OBP records at the Drake Passage, *Meredith et al.* (2004) estimated the interannual variation of ACC transport. In recent years, there are many long-term monitoring programs conducted at the passage, such as the cDrake experiment (*Donohue et al.*, 2016). This experiment contains 46 Current and Pressure-recording Inverted Echo Sounders (CPIES) sites moored across the Drake Passage from November 2007 to November 2011 (*Chereskin et al.*, 2012), continuously providing hourly observations of OBP

and near-bottom current velocities. Based on these moored instrumentations, *Donohue et al.*(2016) examined the mean ACC transport at the Drake Passage. In general, however, these moored instrumentations are still too sparse compared to vastness of the Southern Ocean, and their continuous records are usually no more than a few years.

The launch of the Gravity Recovery and Climate Experiment (GRACE) mission provides a unique way to monitor global OBP variabilities (*Tapley et al.*, 2004), which has greatly advanced the understanding of oceanic dynamics, such as the global mean sea level budget (*Chambers et al.*, 2017) and regional sea level change (*Cheng and Qi*, 2010). Recently, OBP data based on GRACE satellites are also used to estimate the basin-wide oceanic transports on seasonal to interannual scales (*Liau and Chao*, 2017; *Makowski et al.*, 2015; *Mazloff and Boening*, 2016), and even the deep ocean transport through the Luzon Strait (*Zhu et al.*, 2022). Thus, the OBP data from GARCE satellites have already played an unprecedented role in oceanic transport estimation, and, therefore, long-term sustained monitoring of ocean transports seems achievable.

Recent studies also noted some uncertainties in GRACE products, such as discrepancies of OBP estimations among different GRACE products (*Blazquez et al.*, 2018; *Chambers and Bonin*, 2012), and the aliasing errors of GRACE products within the periods less than 60 days (*Quinn and Ponte*, 2011). Given the active mesoscale activities in the Southern Ocean (*Rintoul and Sokolov*, 2001), an assessment of accuracies of different GRACE OBP products is needed before calculating ACC transport.

In this paper, variations in the ACC transport are calculated by using both in-situ OBP data and GRACE OBP products. The remainder of this paper is organized as follows. Data and methods are presented in Section 2. In Section 3, we assess the performance of GRACE products, and reveal the accelerating ACC transport under climatic change. In Section 4, we discuss the

potential mechanisms of the ACC acceleration.

2. Data and methods

In this study, monthly OBP data from five GRACE products are used. Three of them are based on spherical harmonic solutions from Center for Space Research (CSR), Jet Propulsion Laboratory (JPL), and GeoForschungsZentrum Potsdam (GFZ), named as CSR RL06.3, JPL RL06.3 and GFZ RL06.3 products, respectively. The other two products are based on mascon solutions (separating the Earth into equal-area mass concentration cells) from CSR and JPL, named as CSR RL06.2 M and JPL RL06.2 M products, respectively. In this study, the above five GRACE products are referred to as CSR-HR, JPL-HR, GFZ-HR, CSR-MAS and JPL-MAS, respectively. The CSR-HR, JPL-HR and GFZ-HR have the same spatial grids with the horizontal resolution of 1°×1° (*Chambers and Willis*, 2010). The horizontal resolution of JPL-MAS is 0.5°×0.5° and the resolution of CSR-MAS is 0.25°×0.25°. The grid point locations of the five GRACE products are shown in Figure S1.

In-situ OBP records are obtained from the cDrake experiment. As shown in Figure 2a, 46 CPIES sites cover one meridional (black triangles, C line) and three zonal lines [green triangles, Local Dynamics Array (LDA)]. There are also five CPIESs across the Shackleton Fracture Zone (SFZ; magenta triangles, H array), which were placed during the last year. More detailed information of CPIES records is listed in Table S1.

The daily absolute dynamic topography (ADT) data are obtained from Archiving Validation and Interpretation of Satellite Data in Oceanography (AVISO) with a 0.25°×0.25° horizontal resolution. The bathymetry data is obtained from the ETOPO5 global elevation database, which is on a 5'×5' grid. Surface winds are obtained from ERA5 monthly averaged data obtained from

the Asian-Pacific Data Research Center at the University of Hawaii, with a horizontal resolution of 0.25°×0.25°.

When calculating the monthly-mean values of CPIES records, the hourly records are firstly averaged into daily mean, but the daily data are set as missing values if hourly data account for less than half of the day (Figure S1c). Before doing the analysis of monthly mean, a 30-day low-pass Butterworth filter was applied on the daily data to eliminate the higher-frequency signals. The correlation, root-mean-square error (RMSE), and standard deviation (STD) are used to assess the performance of GRACE products in the ACC transport estimation. Student's *t*-test and Mann-Kendall test are used to test the statistical significance of the correlation coefficient and the trend, respectively.

The Pressure Coordinate Ocean Model (PCOM) is used in this study. The model is based on mass conservation, rather than the Boussinesq approximation, and can therefore directly simulate the OBP variations (*Huang et al.*, 2001; *Zhang et al.*, 2014). The model is initialized from a resting state with the World Ocean Atlas 2009 (WOA09) and is spun-up with the climatological monthly atmospheric forcing (including sea level pressure, surface wind, surface heat flux and fresh water flux) for 600 years. After the 600-years spin-up integration, the monthly atmospheric forcing is used to force the model from January 1990 to December 2018 (see *Cheng et al.* (2021) for a more detailed model setup). The model output has a 1°×1° horizontal resolution and 60 pressure layers, which has been successfully applied examining OBP variations in the Southern Ocean (*Niu et al.*, 2022; *Qin et al.*, 2022; *Xiong et al.*, 2022).

3. Results

Before evaluating the performance of GRACE products on ACC transport estimation, we firstly explored the OBP mesoscale signals by using in-situ records. Figure 2b shows the power

spectrum of daily OBP from CPIES records (30-day low-pass filtered) as a function of frequency. It is obvious that most of the energy is concentrated in the mesoscale range (30-150 days), which cannot be well resolved by the monthly averaged GRACE measurements. Considering the stronger EKE to the north of the PF and weaker EKE to the south, we further calculated the power spectra of daily OBP in the northern (red line in Figure 2b) and southern passages (blue line in Figure 2b), respectively. The result reveals a significant north-south difference: there are intense mesoscale signals in the northern passage but weak in the south, which is consistent with the spatial distributions of the EKE at the Drake Passage (Figure 1).

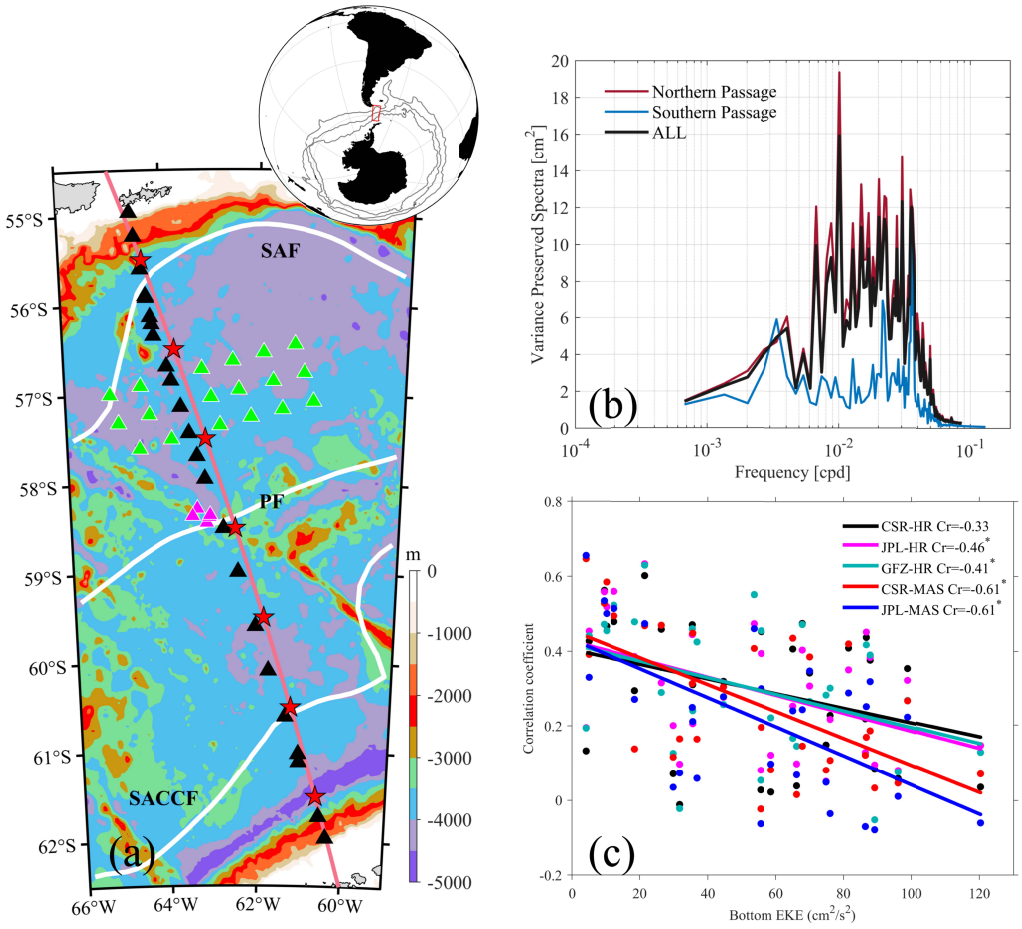

Figure 2. (a) Spatial distributions of 46 CPIES at the Drake Passage. The C line and Local Dynamics Array (including A, B, D, E, F and G arrays) are labelled by black and green triangles, respectively, while H arrays are shown with magenta triangles. White lines

denotes the Subantractic Front (SAF), Polar Front (PF) and Southern ACC Front (SACCF). Red pentagrams are the interpolated site locations studied later. The inset shows the location of the study area (red box). (b) Variance-preserved power spectra as a function of frequency of OBP (30-day low-pass filtered) at the Drake Passage. Black, red and blue lines represent the results in the whole passage, to the north of PF (58.5°S), and to the south of PF, respectively. (c) Scatter plot of bottom EKE and correlation coefficients between CPIES records and GRACE products at each site. Black, magenta, green, orange, and blue dots (regression lines) represent the results using CSR-HR, JPL-HR, GFZ-HR, CSR-MAS, JPL-MAS, respectively. * indicates the 95% confidence level of student's *t*-test.

To explore whether the performance of GRACE products is affected by local mesoscale signals, we calculated the pointwise correlation between monthly averaged CPIES records and five GRACE products. The OBP time series at each CPIES site from GRACE products are obtained by using linear 2-D interpolation. The interpolation has no impact on the extraction of grid data from different horizontal resolution products in this study (not shown). In general, correlation coefficients are the highest in the southern passage and lowest in the Polar Frontal Zone (Figure S2a-2e). Pointwise RMSEs between monthly averaged CPIES records and five GRACE products were also calculated, and the result is consistent with that of the correlation coefficients (not shown). By using bottom velocity anomalies (30-150-days band-pass filtered) from CPIES, the time-mean bottom EKE was calculated at each site, whose spatial pattern well matches that of the correlation coefficients (Figure S2f). In order to show the relationship in a more straightforward way, the scatter plots of bottom EKE and correlation coefficients between GRACE products and CIPES records are shown in Figure 2c. Regression lines reveal the significant negative relationship between the performance of GRACE products and bottom eddy

activities, independent of the different solutions used in GRACE products. The mascon products show slightly higher regression coefficients than spherical harmonics products, indicating that the eddy activities have stronger impacts on GRACE products based on mascon solutions. In general, it could be reasonably deduced that the local mesoscale processes are the key factor for the spatial inconsistency of the performance of GRACE products at the Drake Passage, and that mesoscale processes with high EKE are unfavorable for reproducing the monthly OBP variability in GRACE products. All these need to be considered when calculating ACC transport.

Previous studies have proposed two main methods to estimate the zonal transport anomalies across the selected section based on OBP data (*Makowski et al.*, 2015; *Zhu et al.*, 2022):

$$\Delta T_x = -\frac{1}{\bar{f}\rho_0}\int_{-H}^{0}(P_N - P_S)\,dz \quad (1)$$

$$\Delta T_x = \int_{y_s}^{y_n}\int_{-H}^{0} -\frac{1}{f\rho_0}\frac{\partial P}{\partial y}\,dzdy \quad (2)$$

where f is the Coriolis parameter and ρ_0 is the reference density. H is the topography depth across the section. P_N and P_S are the OBP time series at the northern and southern boundaries, respectively. The difference between Equation (1) and (2) is whether to use a constant Coriolis parameter $\bar{f}$ and whether to integrate the function meridionally. As we mentioned above, the performance of GRACE products is good in the low EKE regions and unreliable in the high EKE regions (such as the Polar Frontal Zone). Thus, Equation (1) is chosen in this study, as the aliasing errors caused by mesoscale activities are considered to be minimal. In order to make the results independent of the spatial resolution of each GRACE product, the monthly in-situ data and all five GRACE products were interpolated onto the same cross section with the same grid points at 1° meridional resolution (red pentagrams in Figure 2a) before calculation.

Figure 3 shows the time series of the calculated ACC transport using in-situ observations

and five GRACE products. First of all, the results using CSR-HR, JPL-HR, and GFZ-HR products are an order of magnitude smaller than those using in-situ observations (grey lines), while the result of CSR-MAS and JPL-MAS products are of the same order of magnitude. In order to more quantitatively demonstrate the performance of the GRACE product on ACC transport estimates, we calculated the STD of each time series from GRACE products and the correlation coefficients between these time series and the in-situ observations. Among all five GRACE products, the CSR-MAS product has the largest correlation coefficient (r=0.62, significant at the 95% confidence level) with observations, and its STD (11.16Sv) is also the closest to observations (11.31Sv). All these results indicate that OBP from the CSR-MAS product is more reliable to monitor the ACC transport variations at the Drake Passage. Therefore, long-term changes of the ACC transport will be estimated using the CSR-MAS product.

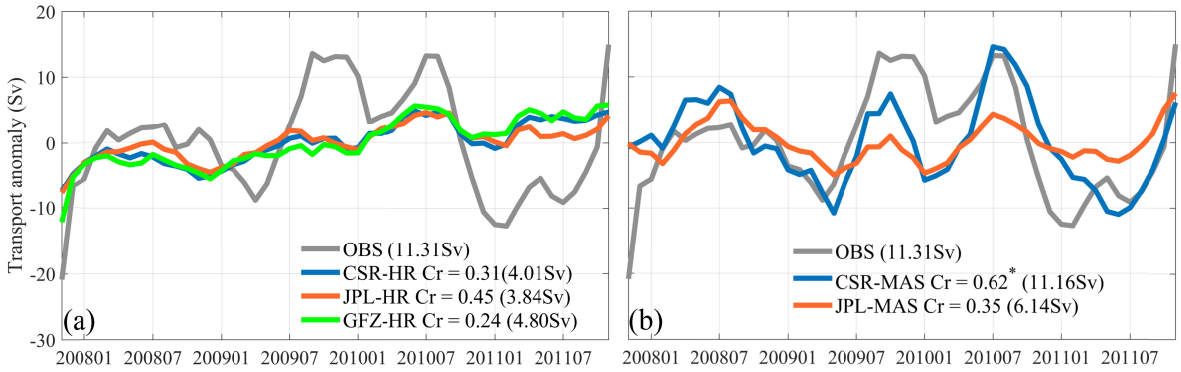

Figure 3. (a) Time series of the ACC transport anomalies smoothed with a five-months moving average filter, calculated using monthly in-situ OBP data (grey line) and GRACE-HR products (color lines). (b) Same as (a) except using GRACE-MAS products (color lines). * indicates the 95% confidence level of student's *t*-test. Values in () indicate the STD of time series.

By using 15-year OBP data from the CSR-MAS product, the ACC transport variations at

the Drake Passage from April 2002 to July 2017 are calculated (the red line in Figure 4a). Despite the interannual variability, there is a clear increasing trend in ACC flow (the pink line, 1.32±0.07Sv year^{-1}, significant at the 95% confidence level). Considering the controlling effect of the westerly wind in the Southern Ocean, the variation in zonal-mean surface wind velocity (averaged between 50°S-65°S) was calculated using ERA5 monthly averaged data (the black line in Figure 4a). The correlation coefficient between zonal-mean wind velocity and the calculated ACC transport is 0.60, significant at the 95% confidence level. The correlation drops to 0.52 when linear trends are removed from both time series (Figure S3). Figure 4b shows the spatial distribution of linear trend of surface winds (arrows) and OBP anomalies (color) at the Drake Passage. It is obvious that the westerly wind has strengthened over the Southern Ocean, and the trend of OBP shows a "dipole structure" at the Drake Passage, increasing in the north and decreasing in the south, which promotes the enhancement of the ACC.

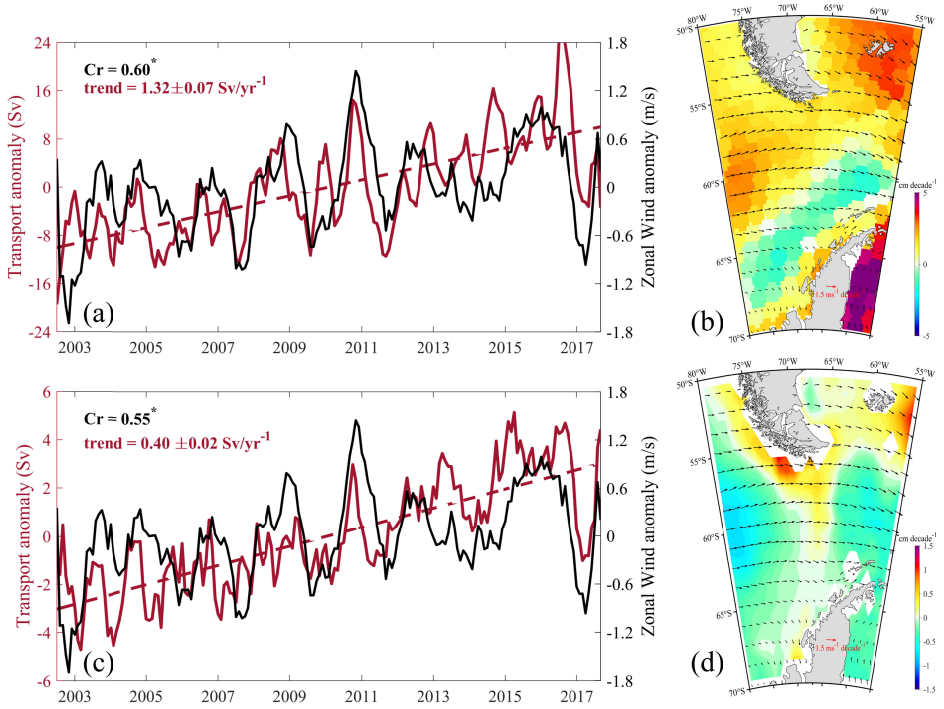

Figure 4. (a) Time series of the ACC transport anomalies using CSR-MAS OBP product (red line) and zonal-mean surface wind (black line) from ERA5 data, smoothed with a

five-months moving average filter. (b) Linear trend of ERA5 surface wind (arrows) and OBP (shading). (c) and (d) are same as (a) and (b) but using PCOM output. * indicates the 95% confidence level of student's *t*-test.

Although the calculated ACC transport shows a good correlation with the zonal-mean wind, there is no direct evidence that the accelerating ACC is mainly caused by the strengthening of westerly winds. Previous studies suggested that the westerly wind dominates the ACC transport variations on timescale from days to years (*Hughes et al.*, 1999; *Meredith et al.*, 2004). On timescales longer than a few years, intrinsic variability in the Southern Ocean readjusts the ACC (*Hogg and Blundell*, 2006). To examine the relationship between ACC trend and the intensifying westerly winds, in this study the PCOM was employed, forced only by surface wind stress from monthly ERA5 data, without changes of heat or freshwater flux. Using the same method as for the GRACE products, we calculated the time series of ACC transport simulated by PCOM. As shown in Figure 4c, a good correlation between ACC transport and zonal wind is found. In addition, the enhancement of the westerly winds leads to increased OBP in the northern passage and decreased OBP in the southern passage along the Antarctic Peninsula (Figure 4d). Such north-south gradient of the OBP in turn accelerates the ACC at the Drake Passage. The ACC transport derived from the PCOM simulation is significantly correlated with that derived from CSR-MAS product (r=0.72, significant at the 95% confidence level, Figure S3), while the amplitude and the rise rate are about one third of those from CSR-MAS product.

Hsu and Velicogna (2017) suggested that glacier loss of the Antarctica could regulate the mass redistribution in the Southern Ocean, leading to significant OBP gradients near the Drake Passage and weak gradients in the other regions (Figure 1 in their paper). Thus, we also

241 compared the zonal-averaged ACC transport variations in the Indian (110^{o}-170^{o}E, 45^{o}-62^{o}S) and
242 Pacific (150^{o}-90^{o}W, 50^{o}-65^{o}S) oceans, with their northern and southern boundaries away from
243 the high EKE regions (orange boxes in Figure 1). As shown in Figure 5, the PCOM result
244 exhibits a good agreement with that from CSR-MAS product, with high correlation coefficients
245 (r=0.59 in the Indian Ocean and r=0.80 in the Pacific, significant at the 95% confidence level),
246 same order of amplitude, and similar trend change of ACC transport. In summary, it could be
247 concluded that the PCOM can well characterize the response of ACC transport to the westerly
248 wind change at the Drake Passage, and the difference in ACC trends between GRACE product
249 and PCOM output may be related to the glacier loss of the Antarctica.
250

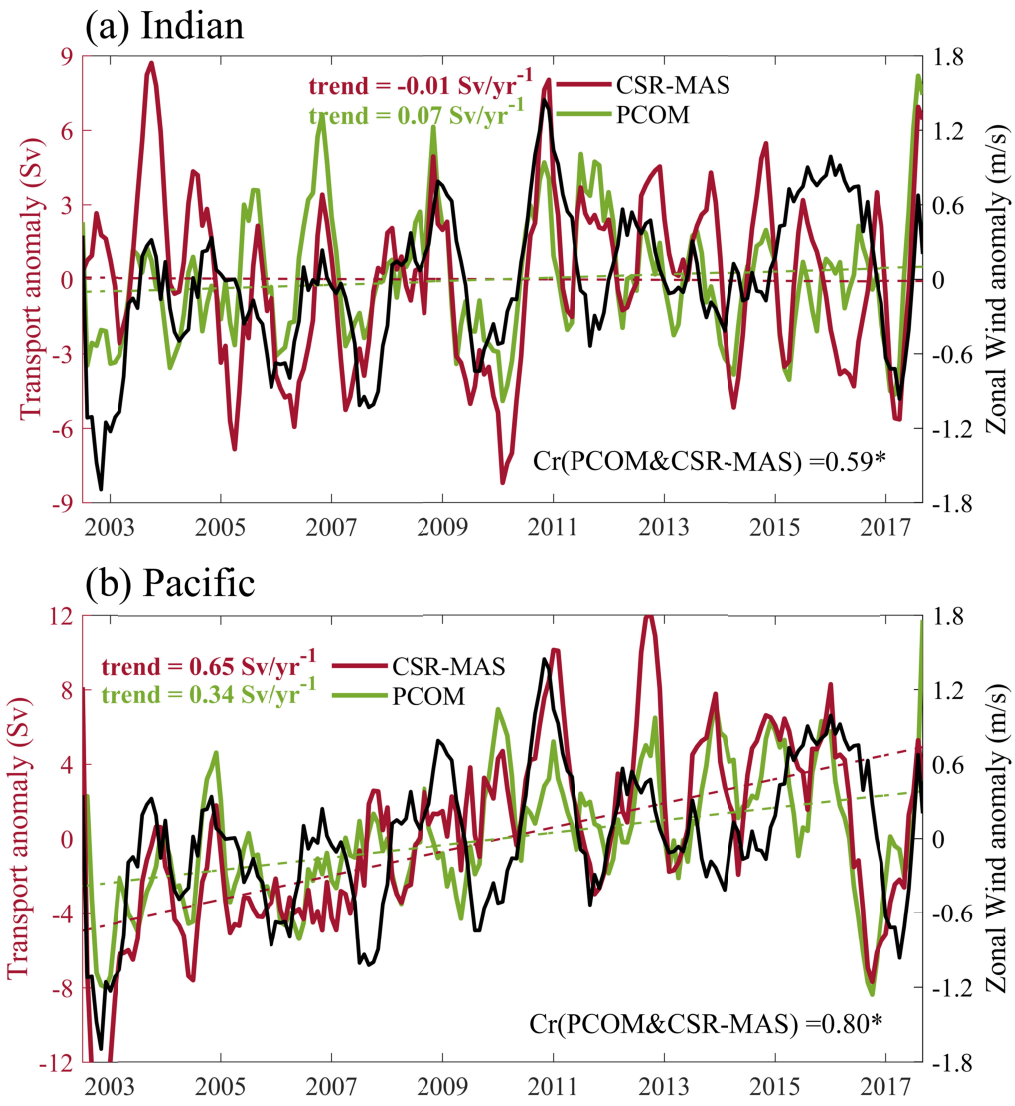

Figure 5. Time series of the ACC transport anomalies calculated using OBP data in the (a) Indian and (b) Pacific oceans, smoothed with a five-months moving average filter. Red and green lines represent the result from CSR-MAS product and PCOM output, respectively. Dash lines represent the linear trend of ACC transport. Black lines in (a) and (b) represent the zonal-mean surface wind variations from ERA5 data, smoothed with a five-months moving average filter. * indicates the 95% confidence level of student's *t*-test.

4. Conclusions and discussions

This study investigates variations of ACC transport at the Drake Passage using in-situ OBP records, five GRACE products, and the PCOM simulation. Our results reveal that the GRACE CSR mascon product closely resembles the in-situ OBP data, and is therefore favorable to estimate ACC transport at the Drake Passage. Based on 15-year CSR mascon product, the changes of ACC transport in the context of climatic change is studied. ACC transport at the Drake Passage shows an obvious increasing trend of 1.32 ± 0.07Sv yr^{-1}. Sensitivity experiment using PCOM indicates that the intensified westerly winds can partially explain the ACC acceleration at the Drake Passage. The glacial loss of Antarctica may account for the residual parts of the acceleration.

Although the PCOM model can partially capture the increasing trend of ACC transport, there are some differences of OBP trends between PCOM results and GRACE measurements. As shown in Figure 4b, except for the southern passage, OBP trends from CSR-MAS product are mostly positive at the Drake Passage, with a maximum value at 75°W, 60°S. In contrast, OBP trends from PCOM are mostly negative in the southern passage, with a minimum value at 75°W, 60°S (Figure 4d). This difference in spatial distribution may be due to the absence of glacier loss in the Antarctica. Thus, the meridional OBP gradient in the model is presumably due to mass redistribution caused by wind-induced Ekman transport. This result confirms previous findings (*Hsu and Velicogna*, 2017) stating that mass redistribution due to glaciers loss accounts for most OBP trend at the Drake Passage during the GRACE era. This can explain the faster increasing trend of the ACC transport estimated from CSR-MAS OBP product.

At present, the response of the ACC to climatic change (changes in westerly wind and buoyancy forcing) has received increasing attention (*Rintoul*, 2018). There is no doubt that in the context of intensified westerly winds, kinetic energies have increased in the Southern Ocean (*Hu*

283 *et al.*, 2020). However, it is still unclear how and where these additional energies are stored.
284 Model-based studies reveal that the ACC transport is insensitive to the increase of the westerly
285 wind (*Downes et al.*, 2011), and the additional energy is transferred into mesoscale eddies
286 (*Marshall et al.*, 2017), which is known as the "eddy saturation" hypothesis (*Munday et al.*,
287 2013). However, based on altimetry crossover measurements and ocean reanalysis product,
288 *Zhang et al.* (2021) found that EKE does not increase coherently across the Southern Ocean.
289 This contradiction may be due to the fact that changes of kinetic energies in the deep ocean are
290 not considered in these studies. Based on OBP data, our results indicate that ACC is accelerating
291 in the deep ocean, at least at the Drake Passage. Therefore, more observational research in the
292 deep Southern Ocean are needed to improve our understanding of energy transport pathways in
293 the Southern Ocean, especially in the context of global warming.

294 **Acknowledgments**

295 This research was supported by the Natural Science Foundation of China (Grant no.41876002)
296 and Postgraduate Research & Practice Innovation Program of Jiangsu Province (grant
297 KYCX22_0585).

298 **Data Availability Statement**

299 The GRACE data are available at https://podaac.jpl.nasa.gov/GRACE and
300 https://www2.csr.utexas.edu/grace/RL06_mascons.html. In-situ bottom pressure records of
301 cDrake experiment are obtained from the University of Rhode Island Web site
302 (http://www.po.gso.uri.edu/dynamics/Drake/index.html). Absolute dynamic topography data are
303 available from the Copernicus Marine Environment Monitoring Service Web site
304 (https://resources.marine.copernicus.eu/product-detail/SEALEVEL_GLO_PHY_L4_MY_008_0
305 47/DATA-ACCESS). The ETOPO5 database is obtained from the National Centers for

306 Environmental Information Web site (https://www.ngdc.noaa.gov/mgg/global/etopo5.HTML).
307 ERA5 monthly averaged wind data are available from Asian Pacific data research center at the
308 University of Hawaii Web site (http://apdrc.soest.hawaii.edu/las/v6/constrain?var=16447).
309

310 **References**

311 Blazquez, A., B. Meyssignac, J. M. Lemoine, E. Berthier, A. Ribes, and A. Cazenave (2018),
312 Exploring the uncertainty in GRACE estimates of the mass redistributions at the Earth
313 surface: implications for the global water and sea level budgets, *Geophysical Journal*
314 *International*, *215*(1), 415-430, doi: 10.1093/gji/ggy293.
315 Chambers, D. P., and J. K. Willis (2010), A Global Evaluation of Ocean Bottom Pressure from
316 GRACE, OMCT, and Steric-Corrected Altimetry, *Journal Of Atmospheric And Oceanic*
317 *Technology*, *27*(8), 1395-1402, doi: 10.1175/2010jtecho738.1.
318 Chambers, D. P., and J. A. Bonin (2012), Evaluation of Release-05 GRACE time-variable gravity
319 coefficients over the ocean, *Ocean Science*, *8*(5), 859-868, doi: 10.5194/os-8-859-2012.
320 Chambers, D. P., A. Cazenave, N. Champollion, H. Dieng, W. Llovel, R. Forsberg, K. von
321 Schuckmann, and Y. Wada (2017), Evaluation of the Global Mean Sea Level Budget
322 between 1993 and 2014, *Surveys In Geophysics*, *38*(1), 309-327, doi:
323 10.1007/s10712-016-9381-3.
324 Cheng, X., N. Ou, J. Chen, and R. X. Huang (2021), On the seasonal variations of ocean bottom
325 pressure in the world oceans, *Geoscience Letters*, *8*(1), doi: 10.1186/s40562-021-00199-3.
326 Cheng, X. H., and Y. Q. Qi (2010), On steric and mass-induced contributions to the annual
327 sea-level variations in the South China Sea, *Global And Planetary Change*, *72*(3), 227-233,
328 doi: 10.1016/j.gloplacha.2010.05.002.

329 Chereskin, T. K., K. A. Donohue, and R. Watts (2012), cDrake: Dynamics and Transport of the
330 Antarctic Circumpolar Current in Drake Passage, *Oceanography*, *25*(3), 134-135, doi:
331 10.5670/oceanog.2012.86.
332 Donohue, K. A., K. L. Tracey, D. R. Watts, M. P. Chidichimo, and T. K. Chereskin (2016), Mean
333 Antarctic Circumpolar Current transport measured in Drake Passage, *Geophysical Research*
334 *Letters*, *43*(22), doi: 10.1002/2016gl070319.
335 Downes, S. M., A. S. Budnick, J. L. Sarmiento, and R. Farneti (2011), Impacts of wind stress on
336 the Antarctic Circumpolar Current fronts and associated subduction, *Geophysical Research*
337 *Letters*, *38*(11), n/a-n/a, doi: 10.1029/2011gl047668.
338 Haumann, F. A., N. Gruber, M. Münnich, I. Frenger, and S. Kern (2016), Sea-ice transport
339 driving Southern Ocean salinity and its recent trends, *Nature*, *537*(7618), 89-92, doi:
340 10.1038/nature19101.
341 Hogg, A. M. C., and J. R. Blundell (2006), Interdecadal Variability of the Southern Ocean,
342 *Journal of Physical Oceanography*, *36*(8), 1626-1645, doi: 10.1175/JPO2934.1.
343 Hsu, C.-W., and I. Velicogna (2017), Detection of sea level fingerprints derived from GRACE
344 gravity data, *Geophysical Research Letters*, *44*(17), 8953-8961, doi:
345 10.1002/2017gl074070.
346 Hu, S., J. Sprintall, C. Guan, M. J. McPhaden, F. Wang, D. Hu, and W. Cai (2020),
347 Deep-reaching acceleration of global mean ocean circulation over the past two decades,
348 *Science advances*, *6*(6), eaax7727, doi: 10.1126/sciadv.aax7727.
349 Huang, R., X. Jin, and X. Zhang (2001), An oceanic general circulation model in pressure
350 coordinates, *Advances in Atmospheric Sciences*, *18*(1), 1-22, doi:
351 10.1007/s00376-001-0001-9.

Hughes, C. W., M. P. Meredith, and K. J. Heywood (1999), Wind-Driven Transport Fluctuations through Drake Passage: A Southern Mode, *Journal of Physical Oceanography*, *29*(8), 1971-1992, doi: 10.1175/1520-0485(1999)029<1971:WDTFTD>2.0.CO;2.

Liau, J. R., and B. F. Chao (2017), Variation of Antarctic circumpolar current and its intensification in relation to the southern annular mode detected in the time-variable gravity signals by GRACE satellite, *Earth Planets And Space*, *69*, 1-9, doi: 10.1186/s40623-017-0678-3.

Makowski, J. K., D. P. Chambers, and J. A. Bonin (2015), Using ocean bottom pressure from the gravity recovery and climate experiment (GRACE) to estimate transport variability in the southern Indian Ocean, *Journal Of Geophysical Research-Oceans*, *120*(6), 4245-4259, doi: 10.1002/2014jc010575.

Marshall, D. P., M. H. P. Ambaum, J. R. Maddison, D. R. Munday, and L. Novak (2017), Eddy saturation and frictional control of the Antarctic Circumpolar Current, *Geophysical Research Letters*, *44*(1), 286-292, doi: https://doi.org/10.1002/2016GL071702.

Mazloff, M. R., and C. Boening (2016), Rapid variability of Antarctic Bottom Water transport into the Pacific Ocean inferred from GRACE, *Geophysical Research Letters*, *43*(8), 3822-3829, doi: 10.1002/2016gl068474.

Meredith, M. P., P. L. Woodworth, C. W. Hughes, and V. Stepanov (2004), Changes in the ocean transport through Drake Passage during the 1980s and 1990s, forced by changes in the Southern Annular Mode, *Geophysical Research Letters*, *31*(21), doi: https://doi.org/10.1029/2004GL021169.

Meredith, M. P., et al. (2011), Sustained Monitoring Of the Southern Ocean at Drake Passage: Past Achievements And Future Priorities, *Reviews of Geophysics*, *49*(4), doi:

10.1029/2010rg000348.

Munday, D. R., H. L. Johnson, and D. P. Marshall (2013), Eddy Saturation of Equilibrated Circumpolar Currents, *Journal of Physical Oceanography*, *43*(3), 507-532, doi: 10.1175/JPO-D-12-095.1.

Niu, Y., X. Cheng, J. Qin, N. Ou, C. Yang, and D. Huang (2022), Mechanisms of Interannual Variability of Ocean Bottom Pressure in the Southern Indian Ocean, *Frontiers in Marine Science*, *9*.

Qin, J., X. Cheng, C. Yang, N. Ou, and X. Xiong (2022), Mechanism of interannual variability of ocean bottom pressure in the South Pacific, *Climate Dynamics*, doi: 10.1007/s00382-022-06198-0.

Quinn, K. J., and R. M. Ponte (2011), Estimating high frequency ocean bottom pressure variability, *Geophysical Research Letters*, *38*(8), n/a-n/a, doi: 10.1029/2010gl046537.

Rintoul, S. R. (2018), The global influence of localized dynamics in the Southern Ocean, *Nature*, *558*(7709), 209-218, doi: 10.1038/s41586-018-0182-3.

Rintoul, S. R., and S. Sokolov (2001), Baroclinic transport variability of the Antarctic Circumpolar Current south of Australia (WOCE repeat section SR3), *Journal Of Geophysical Research-Oceans*, *106*(C2), 2815-2832, doi: 10.1029/2000jc900107.

Roemmich, D., J. Church, J. Gilson, D. Monselesan, P. Sutton, and S. Wijffels (2015), Unabated planetary warming and its ocean structure since 2006, *Nature Climate Change*, *5*(3), 240-245, doi: 10.1038/nclimate2513.

Tapley, B. D., S. Bettadpur, J. C. Ries, P. F. Thompson, and M. M. Watkins (2004), GRACE measurements of mass variability in the Earth system, *Science*, *305*(5683), 503-505, doi: 10.1126/science.1099192.

Thompson, D. W. J., S. Solomon, P. J. Kushner, M. H. England, K. M. Grise, and D. J. Karoly (2011), Signatures of the Antarctic ozone hole in Southern Hemisphere surface climate change, *Nature Geoscience*, *4*(11), 741-749, doi: 10.1038/ngeo1296.

Wearn, R. B., and D. J. Baker (1980), Bottom pressure measurements across the Antarctic circumpolar current and their relation to the wind, *Deep Sea Research Part A. Oceanographic Research Papers*, *27*(11), 875-888, doi: https://doi.org/10.1016/0198-0149(80)90001-1.

Whitworth, T., W. D. Nowlin, and S. J. Worley (1982), The Net Transport of the Antarctic Circumpolar Current through Drake Passage, *Journal of Physical Oceanography*, *12*(9), 960-971, doi: 10.1175/1520-0485(1982)012<0960:TNTOTA>2.0.CO;2.

Xiong, X., X. Cheng, N. Ou, T. Feng, J. Qin, X. Chen, and R. X. Huang (2022), Dynamics of seasonal and interannual variability of the ocean bottom pressure in the Southern Ocean, *Acta Oceanologica Sinica*, *41*(5), 78-89, doi: 10.1007/s13131-021-1878-z.

Zhang, Y., Y. Lin, and R. Huang (2014), A climatic dataset of ocean vertical turbulent mixing coefficient based on real energy sources, *Science China Earth Sciences*, *57*(10), 2435-2446, doi: 10.1007/s11430-014-4904-6.

Zhang, Y., D. Chambers, and X. Liang (2021), Regional Trends in Southern Ocean Eddy Kinetic Energy, *Journal of Geophysical Research: Oceans*, *126*(6), doi: 10.1029/2020jc016973.

Zhu, Y., J. Yao, T. Xu, S. Li, Y. Wang, and Z. Wei (2022), Weakening Trend of Luzon Strait Overflow Transport in the Past Two Decades, *Geophysical Research Letters*, *49*, doi: 10.1029/2021GL097395.